Vietnam Journal of Earth Sciences, 44(1), 109-126, https://doi.org/10.15625/2615-9783/16961

Vietnam Academy of Science and Technology
Vietnam Journal of Earth Sciences
http://www.vjs.ac.vn/index.php/jse

Sea-level rise in Hai Phong coastal area (Vietnam) and its response to ENSO - evidence from tide gauge measurement of 1960-2020

Nguyen Minh Hai[*1,2], Sylvain Ouillon[3,4], Vu Duy Vinh[1]

[1]*Institute of Marine Environment and Resources, VAST, Haiphong City, Vietnam*
[2]*Graduate University of Science and Technology, VAST, Hanoi, Viet Nam*
[3]*UMR LEGOS, University of Toulouse, IRD, CNES, CNRS, UPS, 14 avenue Edouard Belin, 31400 Toulouse, France*
[4]*University of Science and Technology of Hanoi (USTH), VAST, Hanoi 100000, Vietnam*

Received 07 October 2021; Received in revised form 11 December 2021; Accepted 24 February 2022

ABSTRACT

The Hai Phong coastal area (Northwest of the Vietnam East Sea) is prosperous and densely populated, but it is also a place that is considered likely to be severely affected by sea-level rise. Based on the tide gauge measurement data at Hon Dau station during 1960-2020, the sea-level rise trends were analyzed and linked to the El Niño Southern Oscillation (ENSO). The analyses were carried out separately for the whole period (1960-2020) and for the last 19 years (2002-2020) by the Mann-Kendall test and Sen's slope estimator. The Empirical Mode Decomposition method was used to identify the role of ENSO on the water level variability. The results showed a significant sea-level rise trend with a 95% confidence level. The average annual rates of sea-level were 3.56 mm/year and 7.78 mm/year over the periods 1960-2020 and 2002-2020, respectively, indicating a sea-level rise of about 21.4 cm over 60 years and a significant acceleration in sea-level rise recently (14.7 cm over the last 19 years). Sea-level that rose during El Niño events and declined during La Niña, related to ENSO with cycles of 2 and 6.1 years. From 1960 to 2020, ENSO events took four months to impact the sea-level in the Hai Phong coastal area, causing sea-level variability within -3.7 to 7.2 cm over 1972-2020.

Keywords: Sea-level rise, ENSO, interannual sea-level variability, Hon Dau, Hai Phong.

1. Introduction

Sea-level rise (SLR) is one of the most significant effects of climate change. It has drawn international attention because future SLR would cause severe impacts in various parts of the world. While mean sea-level has risen very little over the past 1000 years, recent analyses using historical tide gauge measurements indicated a much higher global SLR (around 2 mm/year) for the 20th century (Douglas 2001, IPCC, 2001, 2007). Moreover, the IPCC (2021) reported that the average rate of SLR has increased faster than expected in a few recent decades: 1.3 mm/year (1901-

[*]Corresponding author, Email: hainm@imer.vast.vn

1971), 1.9 mm/year (1971-2006), and 3.7 mm/year (2006 -2018).

Unlike infrequent large typhoons or earthquakes that can reshape the coastline within hours, the impacts of SLR are typically slow, repetitive, and cumulative (Fitzgerald et al., 2008). Immediate effects include submergence, increased flooding, and saltwater intrusion into surface water, whereas long-term effects will increase coastal erosion and cause saltwater intrusion into groundwater. In addition, coastal wetlands will struggle to keep pace with SLR if sediment supplies are insufficient (Nicholls and Cazenave, 2010). The effects of SLR have significant socioeconomic consequences for the many coastal communities around the world (Small and Nicholls, 2003). Increased coastal erosion as a result of accelerated SLR poses a severe threat to economies worldwide. As the population increases, coastal areas are also likely to experience additional stresses from land-use and hydrological changes (Nicholls et al., 2007). These changes can have devastating effects on coastal habitats further inland, leading to flooding of wetlands, salt contamination of aquifers and agricultural soils, and loss of habitat for fish, birds, plants and many species (Anthoff et al., 2006; Almeida et al., 2016; Church et al., 2013).

The water elevation of the sea varies in time and space due to physical processes, such as tide and waves. Mean sea-level at a given position is defined as the height of the sea surface averaged over a period of time, such as a month or a year, that is long enough to largely eliminate fluctuations caused by tide and waves (Baede, 2007). Mean sea-level also has a spatial distribution on a global scale due to phenomena that dominate regional and local scales. As a result, local mean sea-level changes usually differ from the global oceans. In the Vietnam East Sea, researchers indicated that sea-level has continued to rise (Milne et al., 2009; State Oceanic Administration, 2019).

Besides the long-term rising trend, there are variations in the sea-level (from month to decadal time scale). Tidal oscillations, atmospheric pressure variation, sea surface winds, and ocean circulation patterns, as well as the interaction between the ocean and atmosphere, such as the ENSO (El Niño-Southern Oscillation) phenomena that contribute to the movements and redistribution of seawater on local and/or regional scales (Moon et al., 2015; Muis et al., 2018). Many studies reported that the sea-level variation in many areas of the Pacific Ocean is associated with the ENSO (Enfield and Allen, 1980; Moon et al., 2015; Han et el., 2019; Wang et al., 2018a; Genes et al., 2021). Nerem et al. (2010) reported that detrended global mean sea-level changes are correlated to ENSO occurrences, with positive/negative sea-level anomalies observed during El Niño/La Niña. In the Northwestern Pacific Ocean, the sea-level variation and ENSO have also been investigated. Some results showed that sea-levels at low latitudes, i.e., tropical and subtropical were more responsive to ENSO than at mid-high latitudes (Yuan et al., 2009). Wang et al. (2018a) also reported that ENSO and sea-level anomalies correlations were the largest in the Vietnam East Sea (> 0.6), weaker in the East China Sea (> 0.4 in most areas), and weakest in the Bohai and Yellow Seas (< 0.4), and all correlation coefficients being statistically significant at the 95% confidence level. Wang et al. (2018b) also showed that the significant oscillation periods of ENSO phenomena at a timescale of 4-7 years existed in the sea-level of the Vietnam East Sea with a maximum amplitude of oscillation was 1.5 cm. Notably, based on the Empirical mode decomposition (EMD) method in recent research, Wang et al. (2018a) announced that interannual sea-level change in the Pearl River Estuary responded

to ENSO with ~3-month lag, which caused sea-level to fluctuate from -8.70 to 8.11 cm. Based on the EMD method, Vu Duy et al. (2022) found that ENSO events took ~ 8 months to affect SST at Hai Phong coastal area for 1995-2020, and causing a variation of SST within 1.2°C.

Vietnam is considered one of the most affected countries by climate change (Dasgupta et al., 2009; IPCC, 2007, A.D.B., 2013). Thus, many studies have estimated the manifestations of climate change here, especially SLR. According to Tuong (2001), SLR varied between 1.75 and 2.56 mm/year during 1961-2000 in four coastal stations of Vietnam: Hon Dau (North), Da Nang, Quy Nhon (Center), and Vung Tau (South). MONRE (2016) reported that the mean sea-level of all tide gauges was 2.45 mm/year, and increased significantly to 3.34 mm/year over the period 1993-2014. Recently, Ca (2017) illustrated that sea-level at Hon Dau tide gauge increased by 2.5 mm/year from 1957 to 2012. However, the SLR trend and its variations (at monthly and seasonal scales) in the coastal area of the Vietnam East Sea have not been analyzed in detail. The data have only been updated to 2014. In addition, the relevant studies on the effect of ENSO phenomena on sea-level variation in the coastal area of Vietnam have not demonstrated the contribution of ENSO and its latency to sea-level variation. Therefore, this paper aims to study the sea-level trend (annual, seasonal, monthly) at Hon Dau tide gauge in the Hai Phong coastal area, from 1960 to 2020, with a specific analysis of the recent trend over 2002-2020, as well as the ENSO impact on the sea-level of the study area.

2. Material and methods

2.1. Hai Phong coastal area

The Hai Phong coastal area is located in the western part of the Gulf of Tonkin, with high biodiversity, affluent marine resources, and high economic activities. Based on observations for 60 years (1958-2017) at Hon Dau station, the average air temperature was 23.8°C, with an increasing trend. While the average temperature was below 20°C in the winter, it was above 27°C in summer. Analysis of measurements over 1958-2017 at the Hon Dau station showed that the average annual rainfall was 1563 mm. The rainy season is from May to October, with an average rainfall of 350 mm (Vinh et al., 2018).

The Hai Phong coastal area is strongly affected by its hydrological regime of the Red River (Vinh and Uu, 2013; Lefebvre et al., 2012; Vinh and Thanh, 2014). Red River discharge at Son Tay (near the apex of the Red River delta) has varied over the range 80.5 (2010)-160.7 (1971) $\times 10^9$ m^3 $year^{-1}$, with an average value of 110.0 $\times$ 10^9 m^3 $year^{-1}$. River flow encompasses strong seasonal variations, with 71-79% of the total annual water discharge in the rainy season and only 9.4-18% during the dry season (Vinh et al., 2014).

Hai Phong coastal area is strongly influenced by tidal propagation. Several mechanisms are responsible for the tidal asymmetry, such as the higher wave celerity at high water level than at low water level, and the difference of bottom friction at high and low water levels. As a result, flood tide is shorter than the ebb tide in the Cam-Nam Trieu estuary (Lefebvre et al., 2012). The tidal asymmetry can also be illustrated from water level and water discharge measurements at the hydrologic station in the estuary. While the flood period lasted 9 to 10 hours, the ebb tide lasted 14 to 15 hours at spring tide (Vinh & Ouillon, 2021). The study area is affected by tides that are mainly diurnal, with a range of 2.6-3.6 m in spring tide and about 0.5-1.0 m in a neap tide (Vinh and Hai, 2020).

2.2. Data and methods

Hourly sea-level measurements at the Hon Dau station (20°40'N-106°49'E) (Fig. 1) were collected by the Vietnam Hydro-Meteorological Data and Information Center and analyzed from 1960 to 2020 (61 years) to calculate the sea-level trend. The Hon Dau station is located next to Hon Dau Island (Fig. 1), about 20 km to the Northern border part and 15 km to the Southern border part of Hai Phong coastal area. Therefore, sea-level data at the Hon Dau station can be represented for the coastal area with a radius of 15 to 20 km of Hai Phong coastal area. This study also analyzed data from 2002 to 2020 (19 years) separately to clarify the recent trend.

In addition, monthly mean Oceanic Niño Index (ONI) data for the period 1995-2020 were extracted from the NOAA Center for Weather and Climate Prediction database (http://www.cpc.ncep.noaa.gov). The ONI is used to identify El Niño (warm) and La Niña (cold) events in the Tropical Pacific. The ONI is based on the 3-month moving average of the sea surface temperature (SST) anomaly in the Niño 3.4 region (5°N-5°S, 120°W-170°W). An El Niño event is considered as such when the ONI exceeds the threshold value +0.5°C for at least 5 consecutive months. Conversely, a La Niña event is defined as a period with at least five consecutive months with an ONI below -0.5°C (NOAA, 2020).

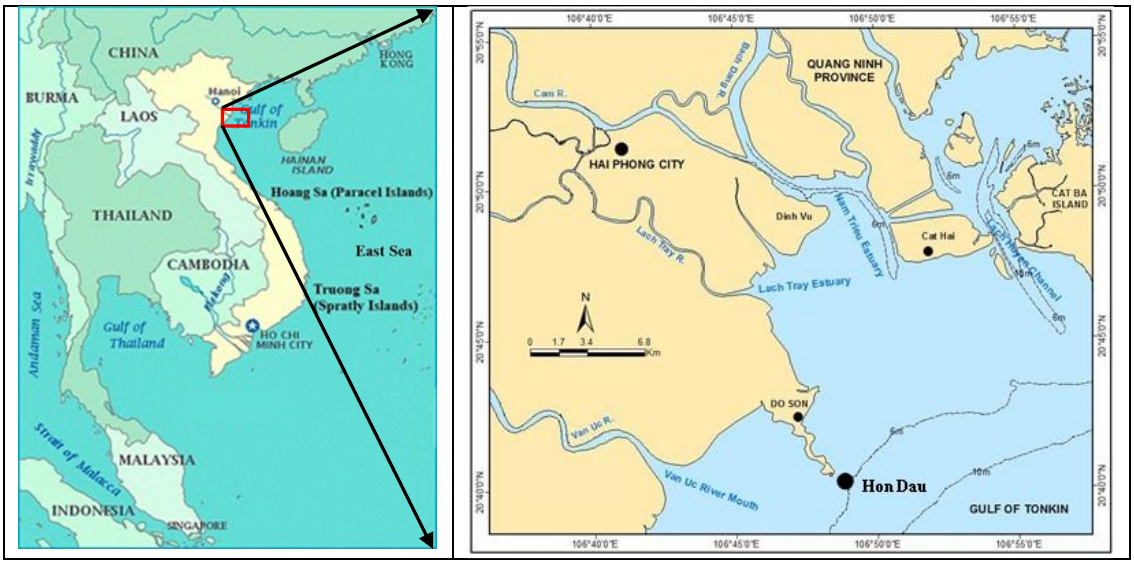

Figure 1. The Hai Phong coastal area and the Hon Dau station (Vu Duy et al., 2022)

The trend is defined as the general movement of a series or the change in the dependent variable over a long period (Webber and Hawkins, 1980). The non-parametric Mann-Kendall (MK) test was derived from Mann (1945) by Kendall (1975). The Sen slope calculation was based on a 1950 proposal by Theil, developed by Sen in 1968 (Sen, 1968; Theil, 1950). This method is commonly used to quantify linear trends in time series (Güner, 2017). In addition, the mean, standard deviation (SD), and coefficient of variation (CV) of sea-level were calculated.

2.2.1. The Mann-Kendall test

This method is widely used in many types of research due to some advantages: not being

affected by missing data and the length of time series; can tolerate outliers in data, and only require data to be independent (Öztopal and Şen, 2017; Wu and Qian, 2017; Kisi, 2015, Shadmani et al., 2012). Combining with the Sen's slope, the MK test have been widely used for detecting trends in hydrometeorological time series such as groundwater (Helsel and Hirsch, 1992), water quality (Hirsch et al., 1982; Hirsch and Slack, 1984; Burn et al., 2012), streamflow (Douglas et al., 2000; Serinaldi et al., 2018), lake level (Chebana et al., 2017), temperature, and precipitation (Sang et al., 2014; Wang et al., 2019), and SLR (Wahl et al., 2011; Chandler and Scott, 2011; Ca, 2017; Ozgenc Aksoy, 2017). MK test and Sen's slope are less sensitive to outliers (Hamed and Rao., 1998; Hamed, 2007), determined by the ranks and sequences of time series rather than the original values. They are robust when dealing with nonnormally distributed data, censored data, and time series with missing values (Hirsch and Slack, 1984), which are commonly encountered in hydrometeorological time series (Duan et al., 2019; Gao et al., 2019; Dong et al., 2019). Therefore, this study employed the Mann-Kendall trend test and Sen's slope to estimate the SLR trend and its significance level in the Hai Phong coastal area.

The Mann-Kendall avoids local maximum values of the data series. The null hypothesis, H_0, is that the data compare the relative magnitude of elements in the data series, a population with independent realizations that do not follow any trend. The alternative hypothesis, H_1, is that the data follow a clear monotonic trend.

The Mann-Kendall S statistic is calculated by analyzing all possible pairs of measurements in the data set. If the earlier measurement is less in magnitude than a later one, S is incremented by one. On the other hand, if an earlier value is greater in magnitude than a later sample, S is decremented by one.

The Mann-Kendall statistic parameter, S is computed as follows:

$$S = \sum_{i=1}^{n-1} \sum_{j=i+1}^{n} sign(X_j - X_i) \quad (1)$$

where X_i and X_j are random variables (divided the given time series X into two variables, as $X_1, X_2, \dots, X_i$, and $X_{i+1}, X_{i+2}, \dots, X_j$).

$$Sign\left(X_j - X_i\right) = \begin{cases} 1 \; if \; X_j - X_i > 0 \\ 0 \; if \; X_j - X_i = 0 \\ -1 \; if \; X_j - X_i < 0 \end{cases} \quad (2)$$

The variance of *S, VAR (S)* is given by

$$VAR(S) = \frac{n(n-1)(2n+5) - \sum_{p=1}^{m} t_p(t_p-1)(2t_p+5)}{18} \quad (3)$$

The standard test statistic Zs is calculated as follows:

$$Z_S = \begin{cases} \frac{S-1}{\sqrt{VAR(S)}} & \text{for } S > 0 \\ 0 & \text{for } S = 0 \\ \frac{S+1}{\sqrt{VAR(S)}} & \text{for } S < 0 \end{cases} \quad (4)$$

where n is the number of data points, m is the number of unique values (without duplicates) and t_p is the frequency of the p^{th} value. If $|Z_s|$ is greater than $Z_{\alpha/2}$, where α represents the chosen significance level (α =10% at the 90% confidence level with $Z_{0.05}$ = 1.65; α =5% at the 95% confidence level with $Z_{0.025}$ = 1.96; α =1% at the 99% confidence level with $Z_{0.005}$ = 2.58), then the null hypothesis is invalid implying that the trend is significant.

A positive value of Z indicates an increasing trend, and a negative value indicates a decreasing trend. Using P-value calculated for Z, H_0 is rejected if $P < \alpha$.

2.2.2. The Sen's slope estimator

Sen (1968) proposed the non-parametric Sen's slope statistics. The slope for each pair of data may be calculated as follows:

$$Q_i = \frac{(X_j - X_k)}{(j-k)} \quad (5)$$

where j=1, ..., N; x_j and x_k are the data values at time j and k (j > k), respectively.

Sen's slope estimator can be calculated as follows:

$$Q_m = \begin{cases} Q[\frac{N+1}{2}] & \text{if N is odd} \\ \frac{Q_{N/2} + Q_{(N+2)/2}}{2} & \text{if N is even} \end{cases} \quad (6)$$

The Q_m sign reflects data trend, while its value indicates the steepness of the trend.

2.2.3. Cross-correlation between ENSO and sea-level variation

To examine the relationship between ENSO and sea-level, cross-correlation analysis was used. For two time series SL(t) and ONI(t) with length n, where t =1, 2…n, the cross-correlation R(τ) at delay τ can be referred as (Ding et al., 2001; Wang et al., 2018a)

$$R(\tau) = \frac{\sigma_{SLONI}(\tau)}{\sqrt{\sigma_{SL}\sigma_{ONI}}} \quad (7)$$

Where: SL is sea-level; $\sigma_{SLONI}(\tau)$ is the lag τ cross-covariance between SL(t) and ONI(t), σ_{SL} and σ_{ONI} are the variance of SL(t) and ONI(t), respectively.

2.2.4. Impacts of ENSO on frequency and magnitude of local sea-level variation

The Empirical mode decomposition (EMD) method was used to identify the impact of ENSO on the sea-level variation. This method adaptively decomposes an input series into several intrinsic mode functions (IMF) having equal numbers of zero-crossing and extrema (or numbers differing at most by one). Envelopes of $E_{min}(t)$ and $E_{max}(t)$ are estimated from interpolation between local minima and maxima, respectively (Huang et al., 2003). The EMD procedure can ascertain the dominant modes in the series SL(t) and then iteratively subtract the less dominant modes that are local mean values in the series $(E_{min}(t)+E_{max}(t))/2$. This procedure is terminated if all the dominant modes are identified. The local mean IMF value extracted is zero.

The detailed procedure can be expressed as:

$$SL(t) = \sum_{j=1}^{M} d_j(t) + r(t) \quad (8)$$

Where r(t) is a monotonic function and reflects the trend of the series SL(t). $\{d_j(t)\}_{j=1}^{M}$ denotes M IMFs within the series. To minimize problems of pseudo - IMF signal and mode confusion, the mirroriing extension method that adds extrema using mirror symmetry was applied to restrain end effects (Rilling et al., 2003).

According to Wu and Huang (2004), the average period of each IMF can be calculated based on the length of original data (n) and the number of peaks:

$$P_k = \frac{n}{n_{pk}} \quad (9)$$

In which, P_k is the average period of IMF k^{th}, n is the length of original data, and n_{pk} is the number of local peak values of the IMF k^{th}.

The EMD method was used to evaluate the impact of ENSO on interannual sea-level variability in the Pearl River Estuary (Wang et al., 2018a), coastal sea-level variability, and extreme events in Cordoba, Colombian Caribbean Sea (Genes et al., 2021).

3. Results

3.1. Temporal variation of the sea-level in Hai Phong coastal area

The measured data at Hon Dau station were analyzed from 1960 and 2020 and given in Fig. 2. The results showed that the average water level in this area was 190.54 cm. They have tended to be high in recent years, especially from 2016 to the present, the average water level was above 202 cm. The

average maximum and minimum sea-levels were 206.1 cm (2017) and 165.2 cm (1963), respectively. The lowest value was in February and March, with about 181 cm, then they gradually increased and reached 208.26 cm in October. The standard deviation (SD) and coefficient of variation (CV) were 8.58 cm and 4.5%, respectively (Table 1).

During 1960 -2020, the maximum monthly water levels were above 201 cm, reaching more than 226 cm in October and November. The lowest monthly water level varies between 152.68 and 179.61 cm. The lowest water level occurred from February to May, with a value below 155 cm. Average monthly water levels tended to be higher in September-November (198-208 cm), especially in October (208 cm). On the other hand, the lowest values were from February to April, with 181-182 cm (Fig. 3, Table 1).

The descriptive statistics of the sea-level, such as the mean, SD, and CV, are presented in Table 1. The SD of the monthly mean sea-level did not differ much from month to month, ranging from 8.73 to 10.69 cm. On the other hand, the CV varied from 4.58 to 5.68% (Fig. 3, Table 1). As shown in Fig. 4, a linear regression described an increasing trend for all months.

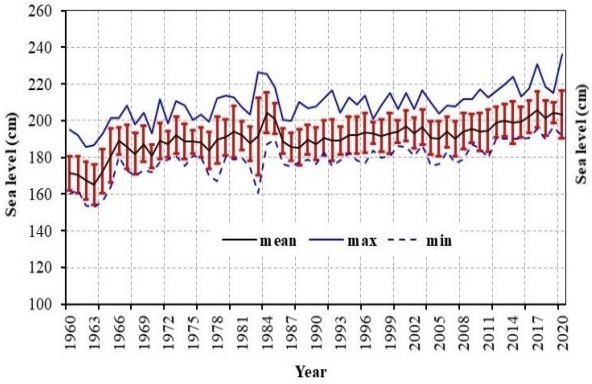

Figure 2. Average annual sea-level at Hon Dau station (1960-2020)

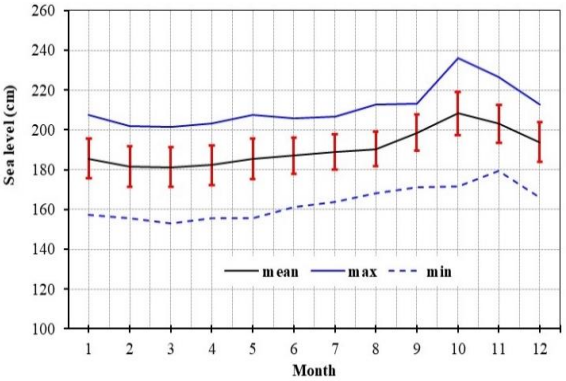

Figure 3. Average monthly sea-level at Hon Dau station (1960-2020)

Table 1. Statistical information of sea-level (cm) at the Hon Dau station (1960-2020)

Month	Maximum	Minimum	Mean	SD (cm)	CV (%)
January	207.50	157.19	185.66	9.78	5.27
February	201.95	155.81	181.56	10.32	5.68
March	201.49	152.88	181.29	10.01	5.52
April	203.39	155.56	182.28	9.82	5.39
May	207.74	155.49	185.57	10.12	5.45
Jun	205.71	161.13	187.01	9.07	4.85
July	206.65	163.76	188.88	8.86	4.69
August	212.67	168.33	190.43	8.73	4.58
September	213.34	171.25	198.61	9.23	4.65
October	236.05	171.79	208.26	10.69	5.14
November	226.66	179.61	203.12	9.46	4.66
December	212.73	166.20	193.85	9.82	5.07
Average	206.06	165.23	190.54	8.58	4.50

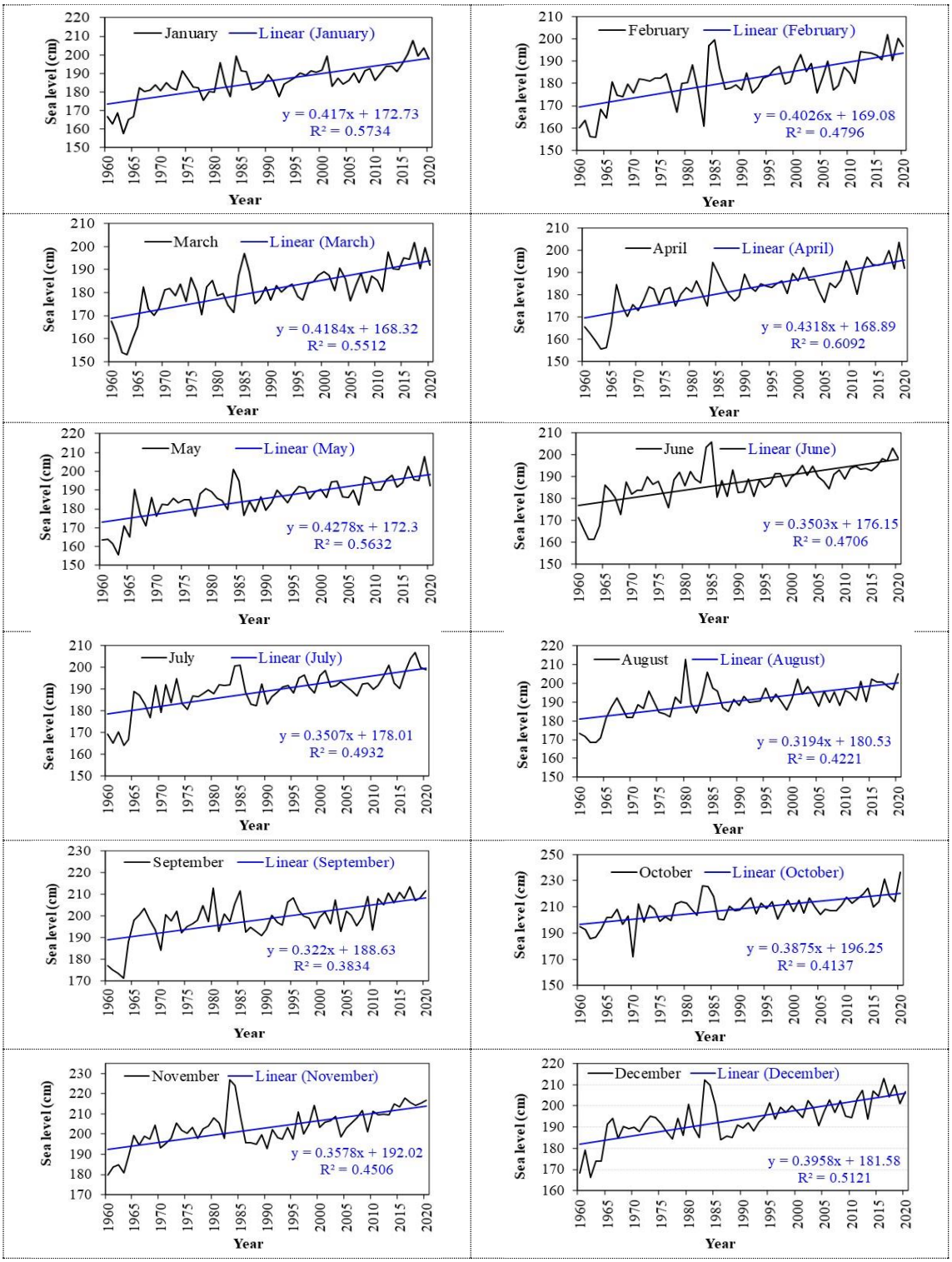

Figure 4. Monthly average sea-level at Hon Dau station (1960-2020)

3.2. The trend of sea-level in Hai Phong coastal area

The sea-level trend was calculated at the Hon Dau station for the periods 1960-2020 and 2002-2020. The results of the Mann-Kendall test on the monthly data are presented in Tables 2 and 3. The *P*-values for all months were approximately zero in 1960-2020 and ranged from 0.00001 to 0.04 in 2002-2020, which was below the considered significance level α of 0.05. Therefore, the H_0 hypothesis was rejected. The rejection of the null hypothesis means the presence of a trend in the series is statistically significant. The results showed a significant positive trend ($Z>0$) for all months and over the periods 1960-2020 and 2002-2020. This means that the mean sea-level has been and tends to rise along the Hai Phong coastal area.

Table 2. The trend of sea-level rise (mm/year) in Hai Phong coastal area (1960-2020)

Month	P-value	Z-stat	Rate of sea-level	Trend
January	0	6.68	3.91	Significant
February	0	5.82	3.93	Significant
March	0	6.37	4.05	Significant
April	0	6.78	4.07	Significant
May	0	6.61	4.06	Significant
June	0	6.33	3.11	Significant
July	0	5.83	3.13	Significant
August	0	5.77	3.13	Significant
September	0	4.64	2.90	Significant
October	0	5.53	3.56	Significant
November	0	6.24	3.81	Significant
December	0	6.17	3.88	Significant
Dry season	0	7.16	**3.92**	Significant
Rainy season	0	6.64	**3.01**	Significant
Average	0	7.66	**3.56**	Significant

Using Sen's approach, the sea-level change (in mm per year) of each time series exhibits a statistically significant monotonic trend (Tables 2 and 3). The monthly average rate from 1960 to 2020 varied from 2.90 mm/year to 4.07 mm/year, which was lower than that from 2002 to 2020. While they were highest from March to May (transition season), with values of 4.05-4.07 mm/year, the lowest value was 2.90 mm/year in September (rainy season).

During the period 2002-2020, the highest monthly trend was observed in January with a rate of change of 10.28 mm/year, while the lowest trend was observed in August, with 4.41 mm/year. In the other months, the rate of sea-level change varied from 4.81 mm/year to 8.93 mm/year. Between 1960 and 2020, the difference in monthly sea-level rates was only 1.17 mm/year, which was about five times smaller than in 2002-2020.

Table 3. The trend of sea-level rise (mm/year) in Hai Phong coastal area (2002-2020)

Month	P-value	Z-stat	Rate of sea-level	Trend
January	0.00001	4.34	10.28	Significant
February	0.0032	2.94	8.93	Significant
March	0.005	2.8	8.37	Significant
April	0.002	3.08	8.86	Significant
May	0.04	2.03	4.81	Significant
June	0.006	2.73	4.88	Significant
July	0.004	2.87	6.09	Significant
August	0.025	2.24	4.41	Significant
September	0.0026	3.01	7.96	Significant
October	0.0016	3.15	9.45	Significant
November	0.0001	3.85	7.40	Significant
December	0.036	2.1	5.51	Significant
Dry season	0.00012	3.85	**8.88**	Significant
Rainy season	0.0016	3.15	**5.50**	Significant
Average	0.00004	4.13	**7.78**	Significant

The study area is affected by the Red river system, whose river discharge is minimum in the dry season (December, January and February) and maximum in the rainy season (June, July and August) (Vinh et al., 2014). We applied the Mann-Kendall method to test the trend and calculated Sen's slope to distinguish between SLR in the dry and rainy seasons. An increasing seasonal trend was detected for both periods ($Z>0$), with Z-stat greater than $Z_{0.005}$ = 2.58, indicating a significant trend at the 99% confidence level. Over 1960-2020, the SLR in the dry season was 3.92 mm/year, which was 0.91 mm/year higher than in the rainy season. Over 2002-2020, it is 8.88 mm/year in the dry season and

5.50 mm/year in the rainy season. The SLR was higher in the dry season than in the rainy season in both periods.

Table 2 and 3 also indicate an annual increasing trend at the 99-100% confidence level (Z>0, Z-sta > $Z_{0.005}$ = 2.58). The average annual rate of SLR was 3.56 mm/year in 1960-2020, lower than the recent period 2002-2020 (7.78 mm/year), which shows that the SLR is increasing.

3.3. Relationship between the sea-level and ENSO phenomena

Based on the EMD method, IMF signals were identified from the time series of sea-level at the Hon Dau station (Fig. 5).

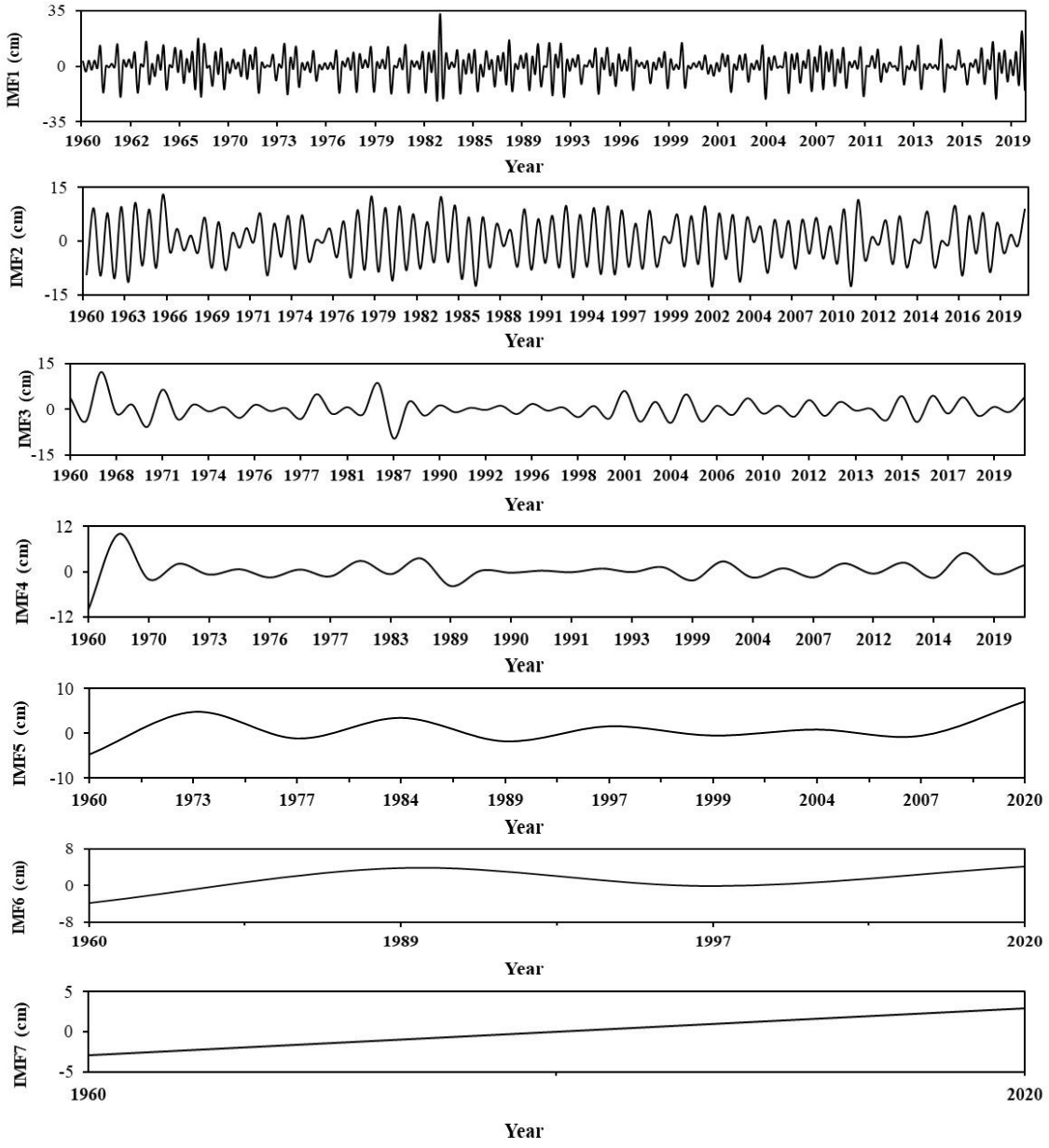

Figure 5. Intrinsic mode function (IMF) signals identified by EMD of sea-level at Hon Dau Station

The period of each IMF signal has been defined: IMF1 shows a period oscillation of around 2.2 months, IMF2 presents typical oscillations of 5.2 months, IMF3 presents typical oscillations of around 11.6 months, IMF4 oscillates mainly between frequencies of 24 months (2 years), IMF5 ranges from 73.2 months (6.1 years), IMF6 ranges about 15.3 years, and IMF7 has a period oscillation of around 30.5 years. The periods of these signals ranged from seasonal (0.2 and 0.4 years), annual (0.97 years), interannual (2.0, 6.1 years), and decadal timescales (15.3 and 30.5 years). Among them, the periods of interannual variation, 2.0-years for IMF4 and 6.1-years for IMF5, were within the El Niño/La Niña cycle of 2-7 years. Two of these signals IMF4 and IMF5 had a range of around 20 cm and 9 cm, respectively (Fig. 5).

For comparison purposes, in accordance with previous studies (Wang et al., 2018a; Genes et al., 2021), a new signal was created from the sum of the IMF4 and IMF5 signals to represent the signal of sea-level response to ENSO, which was called IMF4.5.

The relationship between IMF4.5 and ONI was determined by using the cross-correlation coefficient. The results (Fig. 6a) indicated a high correlation between the two signals (maximum of 0.27, exceeding the 95% lower (-0.04) and upper (0.04) confidence thresholds), and after 4-month delay of the ONI. Considering the results of the cross-correlation analysis, a comparison was made between the IMF4.5 mode and the ONI delayed by 4 months. Figure 6b illustrates the results that IMF4.5 shows similar patterns of variability to the ENSO phenomena: presenting high values as a result of the occurrence of El Niño events (1965-1966, 1986-1987, 2004-2005, 2014-2015, and 2018-2019) and low values related to the occurrence of La Niña events (1983-1984, 1988-1989, 2005-2006, 2016-2017). IMF3 and IMF4 were identified in the EMD analysis, with around -10-10 cm, representing the effect of the ENSO phenomenon on the sea-level at the Hon Dau station. The total influence of ENSO contributed a maximum of about 20 cm (-10 to 10cm) on the sea-level at this region (Fig. 6b).

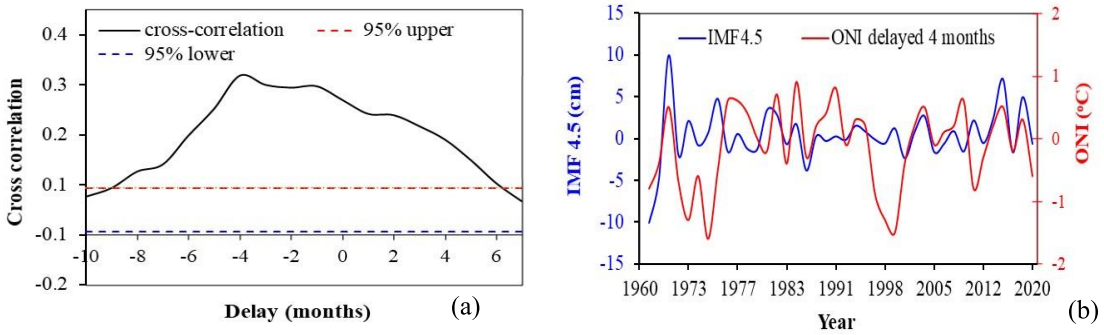

Figure 6. Relationship between sea-level and the ENSO phenomena. (a) Cross-correlation of IMF4.5 and ONI (b) Comparison of IMF 4.5 with ONI delayed by 4 months

4. Discussions

4.1. Sea-level rise

This study focuses on the analysis of in-situ tidal gauge measurements at the Hon Dau station over different periods. All months showed a statistically significant increasing trend ($p < 0.05$). The average rate of SLR during the period 2002-2020 was 7.78 mm/year, higher from 4.22 mm/year than

during the period 1960-2020 (3.56 mm/year), indicating a rise of about 21.4 cm over 60 years (14.7 cm over the last 19 years) and a significant acceleration in SLR recently.

The trend of SLR is consistent with the research results of the Ministry of Natural Resources and Environment (MONRE, 2016), Ca (2017), and Huan (2016) at the Hon Dau station. Note, however, that the value of SLR over the period 1960-2020 was slightly lower than the result obtained by Ca (2017) for the period 1957-2012 (3.78 mm/year) and higher than the calculation by Huan (2016) from in situ data of the Hon Dau station between 1957 and 2015 (2 mm/year). Our result was higher than the calculation obtained over the period 1960-2014 at the Hon Dau station (2.02 mm/year) and the average water level rise at all coastal stations of Vietnam in the period 1993-2014 (3.5 mm/year) (MONRE, 2016). These results provide further evidence, if needed, of the SLR in the Hai Phong coastal area. Moreover, the manifestation of climate change (SLR) has been more evident in recent years.

In addition, global SLR also shows considerable variability in its rate. While mean sea-level has risen very little over the past 1000 years, recent analyses using historical tide gauge measurements indicated a much larger global SLR, of the order 1.5 to 2.0 mm/year for the 20th century (Douglas, 2001). This increase was10 times higher than in previous centuries (Cheikh et al., 2021). Church and White (2006) reported a noticeable increase in the global mean sea-level rate. While it only rose by about 1.6 mm/year in 1880-2009, it significantly increased for 1993-2009, with 3.2 ± 0.4 mm/year and 2.8 ± 0.8 mm/year from satellite and in-situ data, respectively. The IPCC report (2013) indicated that the global average SLR was 1.7 mm/year between 1901 and 2010, 2.0 mm/year between 1971 and 2010, and 3.2 mm/year between 1993 and 2010. The latest IPCC report (2021) updated these figures and indicated that the average rate of sea-level had increased faster than expected in recent decades: 1.3 mm/year over 1901-1971, 1.9 mm/year over 1971-2006, and 3.7 mm/year for 2006 -2018. SLR is subject to considerable interest in the current context of global warming. The reasons for this rise result from two major processes: the thermal expansion of the ocean caused by variations in the thermal content of the ocean and the inflow of freshwater into the ocean caused by the melting of the polar ice caps and mountain glaciers, as well as potential exchanges with continental water reservoirs (Cazenave et al., 2018; Cogley, 2009; Oerlemanns et al., 2007). In the short term, SLR fluctuates partly due to volcanic eruptions. The volcanic eruptions of Mt Agung in 1963, El Chichon in 1982, and Mt Pinatubo in 1991 were likely to have contributed to the small drops of sea-level in the next few years (Church et al., 2006; Gregory et al., 2006; Domingues et al., 2008).

4.2. Impact of the ENSO phenomena

Like other marine regions in the Pacific Ocean, the coastal area of Hai Phong in particular and the Vietnam East Sea, in general, are also clearly affected by the ENSO phenomena, which are often characterized by temperature anomalies in the tropical Pacific. This phenomenon can affect global temperature, atmosphere pressure, weather patterns, and reflect large-scale atmosphere pressure fluctuations between the western and eastern tropical Pacific through the Walker circulation (Webster and Yang, 1992). Therefore, the seawater level is one evident factor affected by ENSO (Barnard et al., 2015; Becker et al., 2012; Miles et al., 2014; Zhang & Church, 2012). In our study, the ENSO phenomena have clearly affected the variability of sea-level in Hai Phong coastal area. The biggest values of IMF4.5 (changed from around -10 to 10 cm) between 1960 and

1971 (Fig. 6b) were directly related to the rise of the annual water level after 1963 to 1966 (Fig. 3). Moreover, the Hon Dau station is located very close to the Van Uc River mouth, about ten kilometers. Therefore, water elevation may have been influenced by fluvial water of the historical Red River Delta flood in 1971. So, these results are also consistent with a report that decadal trends in the global reconstruction of sea-level vary from 0 to 4 mm/year during the period 1950-2000, with a maximum during the 1970s (White et al., 2005).

During the period 1972-2020, the effect of ENSO on sea-level at the Hon Dau station was smaller than the 1960-1971, and mainly between -3.7 to 7.2 cm. In the relevant study conducted by Genes et al. (2021) in Moñitos, Cordoba (Colombian Caribbean Sea), their results also showed the trend of the SLR (from Sen's slope) of about 3.9 mm/year, the contribution of ENSO (by the IMF4.5) to water level variation in this area of around 8 cm. On the other hand, based on the EMD method, Wang et al. (2018a) found the contribution of the ENSO phenomenon on interannual sea-level variability in the Pearl River Estuary for 1953-2013 was around from -8.70 to 8.11 cm. In our study, a good agreement (cross-correlation = 0.27, Fig. 6a) between the two signals (IMF4 and ONI) after a 4-month delay of the ONI indicated that it took 4 months for the tropical ENSO to affect sea-level in the Hai Phong coastal area. Meanwhile, relevant research in Moñitos, Genes et al. (2021) reported that the highest cross-correlation (0.65) between IMF4.5 and the ONI occurred after a 5-month. Wang et al. (2018a) also showed that sea-level in the Pearl River Estuary responded to ENSO with around 3-month lag, and the maximum correlation of ONI and local sea-level anomalies from tide gauge station was 0.38. The above analysis results show a certain match between the results of our study and the previous related research results (Wang et al., 2018a; Genes et al., 2021).

In this study, two IMFs signals have shown that sea-level variability at around 2.0 years (IMF4, Fig. 5) and 6.1years (IMF5, Fig. 6) can be connected to the ENSO index. These results are slightly different from previously related publications. By the data in 1953-2013, Wang et al. (2018a) also found two IMFs signals connected to the ENSO phenomena at the Pearl River Estuary: 3.56-year for IMF4 and 5.02-year for IMF5. On the other hand, based on the analysis from measure data for 1993-2015 at Moñitos, Genes et al. (2021) indicated that three IMFs signal possibly related to the impact of the ENSO on sea-level: 1.0-1.5 years for IMF4, 2.7-3.3 years for IMF5, and 2.6-6.0 years for IMF6. The above results show that the sea-level variability with different cycles related to ENSO is different in the regions. This was confirmed in some previous research (Wang et al, 2018; Wang et al., 2018b; Genes et al., 2021).

5. Conclusions

This study estimated the mean sea-level change in the Hai Phong coastal area from the in-situ data of the Hon Dau station for 1960-2020 and 2002-2020. The Mann-Kendall test was performed to identify statistically significant trends in these series. The results showed an increasing sea-level with a 95-100% confidence level. The magnitudes of the seasonal changes were estimated by Sen's approach. The rates of mean sea-level were 3.56 mm/year and 7.78 mm/year from 1960 to 2020 and from 2002 to 2020, respectively, indicating a much faster rising trend in recent decades. This trend was also observed for each month of the year, with a more marked increase in the dry season than in the wet season. Over the period 1960-2020, the average rates of SLR on a month-by-month basis did not differ significantly, with a

difference of less than 1.17 mm/year. However, this difference increased dramatically between 2002 and 2020 to 4.41 mm/year.

Interannual sea-level change in the Hai Phong coastal area was related to ENSO, which was around 2.0 (IMF4) and 6.1-years'cycle (IMF5). A new signal was created from the sum of these signs, which we have called IMF4.5, representing the ENSO phenomenon's effect on the sea-level variation in the study area. The maximum correlation between it and ONI was 0.27, after 4 months with respect to the occurrence of the ENSO phases. Between 1960 and 2020, ENSO events took 4 months to maximum impact on the sea-level in the Hai Phong coastal area, causing sea-level variability within 20 cm for 1960-1971 and -3.7 to 7.2 cm for 1972-2020.

The sea-level at the Hon Dau station, a tidal gauge station with the longest and best data series in the coastal area of Vietnam, showed significant rises and inter-annual variabilities. These variabilities were significantly affected by climate change and ENSO events. The results of this study provide important insights for SLR prediction in the study area. The ENSO effects should also be considered when implementing inter-annual predictions in the Hai Phong coastal area.

Acknowledgments

This study is benefited from the support of VAST05.05/21-22, NĐT.97.BE/20 and NVCC23.01/22-23 projects. This paper is also a contribution to the LOTUS International Joint Laboratory (http://lotus.usth.edu.vn).

Reference

A.D.B., 2013. Vietnam: Environment and Climate Change Assessment. https://www.adb.org/documents/viet-nam-environment-and-climate-change-assessment.

Almeida B.A., Mostafavi A., 2016. Resilience of infrastructure systems to sea-level rise in coastal areas: impacts, adaptation measures, and implementation challenges, Sustainability, 8(11), 1115. https://doi.org/10.3390/su8111115.

Anthoff D., Nicholls R.J., Tol R.S.J., Vafeidis A.T., 2006. Global and regional exposure to large rises in sea-level: a sensitivity analysis. Tyndall Centre for Climate Change Research, 96, 31.

Baede A.P.M., 2007. Annex I glossary. In Climate Change 2007: The Physical Science Basis. Contribution of Wo/rking Group I to the Fourth Assessment Report of the Intergovernmental Panel on Climate Change (eds. Solomon S., Qin D., Manning M., Chen Z., Marquis M., Averyt K.B., Tignor M. and Miller H.L.). Cambridge University Press, Cambridge, 941-954.

Barnard P.L., et al., 2015. Coastal vulnerability across the Pacific dominated by El Niño/Southern Oscillication. Nature Geoscience, 8 (September), 801-808. https://doi.org/10.1038/NGEO2539

Becker M., Meyssignac B., Letetrel C., Llovel W., Cazenave A., Delcroix T., 2012. Sea level variations at tropical Pacific islands since 1950. Global and Planetary Change, 80-81, 85-98. https://doi.org/10.1016/j.gloplacha.2011.09.004

Burn D.H., Hannaford J., Hodgkins G.A., Whitfield P.H., Thorne R., Marsh T., 2012. Reference hydrologic networks II. using reference hydrologic networks to assess climate-driven changes in streamflow. Hydrol. Sci. J., 57, 1580-1593. Doi: 10.1080/02626667.2012.728705.

Ca V.T., 2017. A Climate Change Assessment via Trend Estimation of Certain Climate Parameters with In Situ Measurement at the Coasts and Islands of Viet Nam. Climate, 5, 36. https://doi.org/10.3390/cli5020036.

Cazenave A., et al., 2018. Global Sea-Level Budget 1993-Present. Earth System Science Data, 10, 1551-1590. https://doi.org/10.5194/essd-10-1551-2018.

Chandler R.E., Scott E.M., 2011. Statistical Methods for Trend Detection and Analysis in the Environmental Sciences. John Wiley. Chichester, U. K., 368p.

Chebana F., Aissia M.A.B., Ouarda T.B.M.J., 2017. Multivariate shift testing for hydrological variables,

review, comparison and application. J. Hydrol., 548, 88-103. Doi: 10.1016/j.jhydrol.2017.02.033.

Church J.A., White N.J., 2006. A 20th century acceleration in global sea-level rise. Geophys Res Lett, 33: L10602. Doi: 10.1029/2005GL024826.

Church J.A, Clark P.U., Cazenave A., Gregory J.M., Jevrejeva S., Levermann A., Merrifield M.A., Milne G.A., Nerem R.S., Nunn P.D., Payne A.J., Pfeffer W.T., Stammer D., Unnikrishnan A.S., 2013. Sea Level Change In Climate Change 2013: The Physical Science Basis. Contribution of Working Group I to the Fifth Assessment Report of the Intergovernmental Panel on Climate Change, ed T F Stocker et al. (Cambridge: Cambridge University Press).

Cogley J.G., 2009. Geodetic and direct mass-balance measurements: comparison and joint analysis. Ann. Glaciol., 50, 96-100. https://doi.org/10.3189/172756409787769744.

Dasgupta S., Laplante B., Meisner C., 2009. The impact of sea level rise on developing countries: a comparative analysis. Clim Change, 93(3), 379-388. Doi: 10.1007/s10584-008-9499-5.

Ding X., Zheng D., Chen Y., Zhao J., Li Z., 2001. Sea level changes in Hong Kong from tide gauge measurements of 1954-1999. J. Geodesy, 74, 683-689. https://doi.org/10.1007/s001900000128.

Domingues C.M., Church J.A., White N.J., Gleckler P.J., Wijffels S.E., Barker P.M., Dunn J.R., 2008. Improved estimates of upper-ocean warming and multi-decadal sea-level rise. Nature, 453, 1090-1093. Doi: 10.1038/nature07080.

Dong J., Crow W.T., Duan Z., Wei L., Lu Y., 2019. A double instrumental variable method for geophysical product error estimation. Remote Sens. Environ., 225, 217-228. Doi: 10.1016/j.rse.2019.03.003.

Douglas B.C., 2001. Sea Level Change in the Era of the Recording Tide Gauge. In: Douglas, B., et al., Eds., Sea Level Rise: History and Consequences, Academic, San Diego, 37-64. https://doi.org/10.1016/S0074-6142(01)80006-1.

Douglas E.M., Vogel R. M., Kroll C.N., 2000. Trends in floods and low flows in the United States: impact of spatial correlation. J. Hydrol., 240, 90-105. Doi: 10.1016/S0022-1694(00)00336-X.

Duan Z., Tuo Y., Liu J., Gao H., Song X., Zhang Z., 2019. Hydrological evaluation of open-access precipitation and air temperature datasets using SWAT in a poorly gauged basin in Ethiopia. J. Hydrol., 569, 612-626. Doi: 10.1016/j.jhydrol.2018.12.026

Enfield D.B., Allen J.S., 1980. On the structure and dynamics of monthly mean sea level anomalies along the Pacific coast of North and South America. J. Phys. Oceanogr., 10, 557-578.

Fitzgerald D.M., Fenster M.S., Argow B.A., Buynevich I.V.,2008. Coastal impacts due to sea level rise, Annu. Rev. Earth Planet. Sci., 36, 601-647. https://doi.org/10.1146/annurev.earth.35.031306.140139.

Gao H., Birkel C., Hrachowitz M., Tetzlaff D., Soulsby C., Savenije H.H.G., 2019. A simple topography-driven and calibration-free runoff generation module. Hydrol. Earth Syst. Sci., 23, 787-809. Doi: 10.5194/hess-23-787-2019.

Genes L.S., Montoya R.D., Osorio A.F., 2021. Costal sea level variability and extreme events in Mo˜nitos, Cordoba, Colombian Caribbean Sea. Continental Shelf Research, 228, 104489. https://doi.org/10.1016/j.csr.2021.104489.

Gregory J.M., Lowe J.A., Tett S.F.B., 2006. Simulated global-mean sea-level changes over the last half-millenium. J. Clim., 19, 4576-4591. https://doi.org/10.1175/JCLI3881.1.

Güner B.Ü., 2017. Trend analysis of precipitation and drought in the Aegean region, Turkey: Trend analysis of precipitation and drought, Meteorological Applications, 24(2), 239-249. Available from: https://doi.org/10.1002/met.1622.

Hamed K.H., 2007. Improved finite-sample Hurst exponent estimates using rescaled range analysis. Water Resour. Res., 43, 797-809. Doi: 10.1029/2006WR005111.

Hamed K.H., Rao A.R., 1998. A modified Mann-Kendall trend test for autocorrelated data. Journal of Hydrology, 204(1-4), 182-196. https://doi.org/10.1016/S0022-1694(97)00125-X.

Han W., et al., 2019. Impacts of basin-scale climate modes on coastal sea level: a review. Surv. Geophys., 40(6), 1493-1541.

Helsel D., Hirsch R., 1992. Statistical Methods in Water Resources. Amsterdam: Elsevier.

Hirsch R.M., Slack J.R., 1984. A nonparametric trend test for seasonal data with serial dependence. Water Resour. Res., 20, 727-732. Doi: 10.1029/WR020i006p00727.

Hirsch R.M., Slack J.R., Smith R.A., 1982. Techniques of trend analysis for monthly water quality data. Water Resour. Res., 18, 107-121. Doi: 10.1029/WR018i001p00107.

Huan P.V., 2016. Some parameters of the changeability of the sea levels along the Vietnam coast. VNU Journal of Science: Earth and Environmental Sciences, 32(3S), 90-94 (in Vietnam).

Huang N.E., Wu M.L., Qu W., Long S.R., Shen S.S.P., Zhang J.E., 2003. Applications of Hilbert-Huang transform to non-stationary financial time series analysis. Appl. Stoch. Model. Bus., 19, 245-268. https://doi.org/10.1002/asmb.501.

IPCC, 2001. Climate Change 2001: the Scientific Basis. Contribution of Working Group I to the Third Assessment Report of the Intergovernmental Panel on Climate Change, edited by J. T. Houghton et al., Cambridge Univ. Press, Cambridge, U. K.

IPCC, 2007. Climate change 2007. In: Solomon S, Qin D, Manning M et al (eds) The physical science basis. Contribution of working group I to the fourth assessment report of the intergovernmental panel on climate change. Cambridge University Press, Cambridge.

IPCC, 2013. Climate Change 2013: The Physical Science Basis. Contribution of Working Group I to the Fifth Assessment Report of the Intergovernmental Panel on Climate Change [Stocker, T.F., D. Qin, G.-K. Plattner, M. Tignor, S.K. Allen, J. Boschung, A. Nauels, Y. Xia, V. Bex and P.M. Midgley (eds.)]. Cambridge University Press, Cambridge, United Kingdom and New York, NY, USA, 1535pp.

IPCC, 2021. Climate Change 2021: The Physical Science Basis. Contribution of Working Group I to the Sixth Assessment Report of the Intergovernmental Panel on Climate Change [Masson-Delmotte V., P. Zhai, A. Pirani, S.L. Connors, C. Péan, S. Berger, N. Caud, Y. Chen, L. Goldfarb, M.I. Gomis, M. Huang, K. Leitzell, E. Lonnoy, J.B.R. Matthews, T.K. Maycock, T. Waterfield, O. Yelekçi, R. Yu, and B. Zhou (eds.)]. Cambridge University Press.

Kendall M.G.,1975. Rank correlation methods. 4th Edition, Charles Griffin, London, UK, 272.

Kisi O., 2015. An innovative method for trend analysis of monthly pan evaporations. J. Hydrol., 527, 1123-1129. https://doi.org/10.1016/j.jhydrol.2015.06.009.

Lefebvre J.P., Ouillon S., Vinh V.D., Arfi R., Panche J.Y., Mari X., Van Thuoc C., Torréton J.P., 2012. Seasonal variability of cohesive sediment aggregation in the Bach Dang-Cam Estuary, Haiphong (Vietnam). Geo-Mar. Lett. 2012, 32, 103-121. http://dx.doi.org/10.1007/s00367-011-0273-8.

Mann H.B., 1945. Nonparametric tests against trend. Econometrica, 13, 245-259.

Miles E.R., Spillman C.M., Church J.A., McIntosh P. C., 2014. Seasonal prediction of global sea level anomalies using an oceanatmosphere dynamical model. Climate Dynamics, 1-15. https://doi.org/10.1007/s00382-013-2039-7.

Milne G.A., W.R. Gehrels, C.W. Hughes, M.E. Tamisiea, 2009. Identifying the causes of sea-level change. Nature Geosci., 2, 471-478.

MONRE, 2016. Climate change and sea level rise scenarios for Viet Nam. Hanoi.

Moon J.H., Song Y.T., Lee H.K., 2015. PDO and ENSO modulations intensified decadal sea level variability in the tropical Pacific. J Geophys Res: Oceans 120, 8229-8237. https://doi.org/10.1002/2015JC011139.

Muis S., Haigh I.D., Guimarães Nobre G., Aerts J.C.J.H., Ward P.J., 2018. Influence of El Niño-Southern Oscillation on global coastal flooding. Earth's Future, 6, 1311-1322. https://doi.org/10.1029/2018EF000909.

Nerem R.S., Chambers D.P., Choe C., Mitchum G.T., 2010. Estimating mean sea level change from the TOPEX and Jason altimeter missions. Marine Geodesy, 33(1), 435-446.

Nicholls R.J., Wong P.P., Burkett V.R., Codignotto, J.O., John H., McLean R.F., Ragoonaden, S., Woodroffe C.D., 2007. Coastal systems and low-lying areas, in Climate Change 2007: Impacts, Adaptation, and Vulnerability. Contribution of

Working Group II to the Fourth Assessment Report of the Intergovernmental Panel on Climate Change, edited by M.L. Parry, O.F. Canziani, J.P. Palutikof, P.J. van der Linden, and C. E. Hanson, Cambridge Univ. Press, Cambridge, U. K.

Nicholls R.J.,Cazenave A., 2010. Sea-level rise and its impact on coastal zones, Science, 328(18), 1517-1520. http://dx.doi.org/10.1126/science.1185782.

NOAA, 2020.
https://origin.cpc.ncep.noaa.gov/products/analysis_monitoring/ensostuff/ONI_v5.php. Access on December 31, 2020.

Oerlemanns J., Dyurgerov M., Van de Wal R.S.W., 2007. Reconstructing the glacier contribution to sea-level rise back to 1850, The Cryosphere, 1, 59-65. https://doi.org/10.5194/tc-1-59-2007.

Ozgenc Aksoy, A., 2017. Investigation of sea level trends and the effect of the north atlantic oscillation (NAO) on the black sea and the eastern mediterranean sea. Theor Appl. Climatol., 129, 129-137. https://doi.org/10.1007/s00704-016-1759-0.

Öztopal A., Şen Z., 2017. Innovative Trend Methodology Applications to Precipitation Records in Turkey. Water Resour. Manag., 31, 727-737. https://doi.org/10.1007/s11269-016-1343-5.

Rilling G., Flandrin P., Goncalves P., 2003. On Empirical Mode Decomposition and Its Algorithms. IEEE-EURASIP Workshop on Nonlinear Signal Image Process. NSIP-03. Grado Italy.

Sang Y.F., Wang Z., Liu C., 2014. Comparison of the MK test and EMD method for trend identification in hydrological time series. J. Hydrol., 510, 293-298. Doi: 10.1016/j.jhydrol.2013.12.039.

Sen P.K., 1968. Estimates of the Regression Coefficient Based on Kendall's Tau. Journal of the American Statistical Association, 63(324), 1379. https://doi.org/10.2307/2285891.

Serinaldi F., Kilsby C.G., Lombardo F., 2018. Untenable nonstationarity: an assessment of the fitness for purpose of trend tests in hydrology. Adv.Water Resour., 111, 132-155.
Doi: 10.1016/j.advwatres.2017.10.015.

Shadmani M., Marofi S., Roknian M., 2012. Trend Analysis in Reference Evapotranspiration using Mann-Kendall and Spearman's rho tests in arid regions of Iran. Water Resour Manage, 26, 211-224. Doi: 10.1007/s11269-011-9913-z.

Small C., Nicholls R.J., 2003. A global analysis of human settlement in coastal zones, J. Coastal Res., 19(3), 584-599.
https://www.jstor.org/stable/4299200.

State Oceanic Administration, 2019. China Sea Level Bulletin, State Oceanic Administration, Beijing, China, 2020.

Theil H., 1950. A rank-invariant method of linear and polynomial regression analysis I, II and III. Nederl. Aka. Wetensch., 53, 386-392.

Tuong N.T., 2006. Sea level measurement and sea level rise in Vietnam. Marine Hydrometeorological Centre, Vietnam.

Vinh V.D, Thanh T.D., 2014. Characteristics of current variation in coastal area of red river delta - results of research applied the 3D numerical model. Journal of Marine Science and Technology, 14(2), 139-148.

Vinh V.D., Ouillon S., 2021. The double structure of the Estuarine Turbidity Maximum in the Cam-Nam Trieu mesotidal tropical estuary, Vietnam, Marine Geology, 442, Article 106670.
Doi: 10.1016/j.margeo.2021.106670.

Vinh V.D., Hai N.M., 2020. Coastal zones of the Red river delta and Yangtze river delta. Vietnam Journal of Marine Science and Technology, 19(4), 449-461. https://doi.org/10.15625/1859-3097/12651.

Vinh V.D., Ouillon S., Thanh T.D., Chu L.V., 2014. Impact of the Hoa Binh dam (Vietnam) on water and sediment budgets in the Red River basin and delta. Hydrol. Earth Syst. Sci., 18, 3987-4005. Doi: 10.5194/hess-18-3987-2014.

Vinh V.D., Ouillon S., Uu D.V., 2018. Estuarine Turbidity Maxima and Variations of Aggregate Parameters in the Cam-Nam Trieu Estuary, North Vietnam, in Early Wet Season. Water 2018, 10, 68. http://dx.doi.org/10.3390/w10010068.

Vinh V.D., Uu D.V., 2013. The influence of wind and oceanographic factors on characteristics of suspended sediment transport in Bach Dang estuary. J. Mar. Sci. Technol., 3, 216-226.

Vu Duy V., Ouillon S., Nguyen Minh H., 2022. Sea surface temperature trend analysis by Mann-Kendall test and sen's slope estimator: a study of the Hai

Phong coastal area (Vietnam) for the period 1995-2020. Vietnam Journal of Earth Sciences. https://doi.org/10.15625/2615-9783/16874.

Wahl T., Jensen J., Frank T., Haigh I.D., 2011. Improved estimates of mean sea level changes in the German Bight over the last 166 years, Ocean Dyn., 61, 701-715. Doi:10.1007/s10236-011-0383-x.

Wang H., Liu K., Wang A., Feng J., Fan W., Liu Q., Xu Y., Zhang Z., 2018b. Regional characteristics of the effects of the El Niño-Southern Oscillation on the sea level in the China Sea. Ocean Dynamics, 68, 485-495. https://doi.org/10.1007/s10236-018-1144-x

Wang L., Li Q., Mao X.Z., Bi H., Yin P., 2018a. Interannual Sea level variability in the pearl river Estuary and its response to El Niño-Southern Oscillation. Global Planet. Change, 162, 163-174. Doi: 10.1016/j.gloplacha.2018.01.007.

Wang S., Zuo H., Yin Y., Hu C., Yin J., Ma X., 2019. Interpreting rainfall anomalies using rainfall's nonnegative nature. Geophys. Res. Lett. 46, 426-434. Doi: 10.1029/2018GL081190.

Webber J., Hawkins C., 1980. Statistical Analysis Application to Business and Economics, 626. Harper and Row, New York.

Webster P.J., Yang S., 1992. Monsoon and ENSO: Selectively interactive systems. Quart. J. Roy. Meteor. Soc., 118, 877-926

White N.J., Church J.A., Gregory J.M., 2005, Coastal and global averaged sea level rise for 1950 to 2000, Geophys. Res. Lett., 32, L01601. Doi: 10.1029/2004GL021391.

Wu H., Qian H., 2017. Innovative trend analysis of annual and seasonal rainfall and extreme values in Shaanxi, China, since the 1950s. Int. J. Climatol., 37, 2582-2592. https://doi.org/10.1002/joc.4866.

Wu Z., Huang N.E., 2004. A study of the characteristics of white noise using the empirical mode decomposition method. Proceedings of the Royal Society of London. Series A: Mathematical, Physical and Engineering Sciences, 460, 1597-1611.

Zhang X., Church J.A., 2012. Sea level trends, interannual and decadal variability in the Pacific Ocean. Geophysical Research Letters, 39, L21701. https://doi.org/10.1029/2012GL053240.